Journal of Statistical Physics, Vol. 37, Nos. 1/2, 1984

Homogeneous Periodic Heat Flow via Nonequilibrium Molecular Dynamics*

William G. Hoover,[1] Bill Moran,[2] and James M. Haile[3]

Received March 28, 1984

Two nonequilibrium methods for simulating homogeneous periodic heat flow are applied to 108 three-dimensional soft spheres in both the fluid and face-centered cubic solic phases. Both nonequilibrium methods use irreversible thermodynamics to express heat conductivity in terms of the work required to generate heat flow. The Evans–Gillan method, derived from Green–Kubo theory, correctly reproduces Ashurst's heat conductivities. An approach based on Gauss' principle of least constraint, in which the heat flow is constrained to a fixed value, fails this test. Heat flow is an inhomogeneous, nonlinear function of particle velocities and coordinates. Thus, Gauss' principle cannot be relied upon for treating inhomogeneous nonlinear nonholonomic constraints.

KEY WORDS: Nonequilibrium; molecular dynamics; conductivity; heat flow; irreversible thermodynamics; steady state.

1. INTRODUCTION

Nonequilibrium systems are described by average values of their fluxes (flows per unit area and time) and the forces (usually derived from gradients) which drive them, as well as by distribution functions detailing the spread of these flow values around their means. Transport coefficients relate the fluxes to the forces or gradients which drive them. Nonequilibrium

[1] Department of Applied Science, University of California at Davis-Livermore, and Lawrence Livermore National Laboratory, Livermore, California 94550.
[2] University of California, Lawrence Livermore National Laboratory, Livermore, California 94550.
[3] Department of Chemical Engineering, Clemson University, Clemson, South Carolina 29631.
* Work performed under the auspices of the U.S. Department of Energy by Lawrence Livermore National Laboratory under contract #W-7405-Eng-48. Work performed at U.C. Davis-Livermore with the support of the Army Research Office and the Air Force Office of Scientific Research.

0022-4715/84/1000-0109$03.50/0

molecular dynamics was developed[1] in order to validate the *linear* transport coefficients found[2] by applying Green–Kubo theory in situations close to equilibrium and to provide a way to estimate nonlinear transport in systems far from equilibrium.

Methods of calculation recently introduced by nonequilibrium molecular dynamics involve modifying Newton's equations of motion.

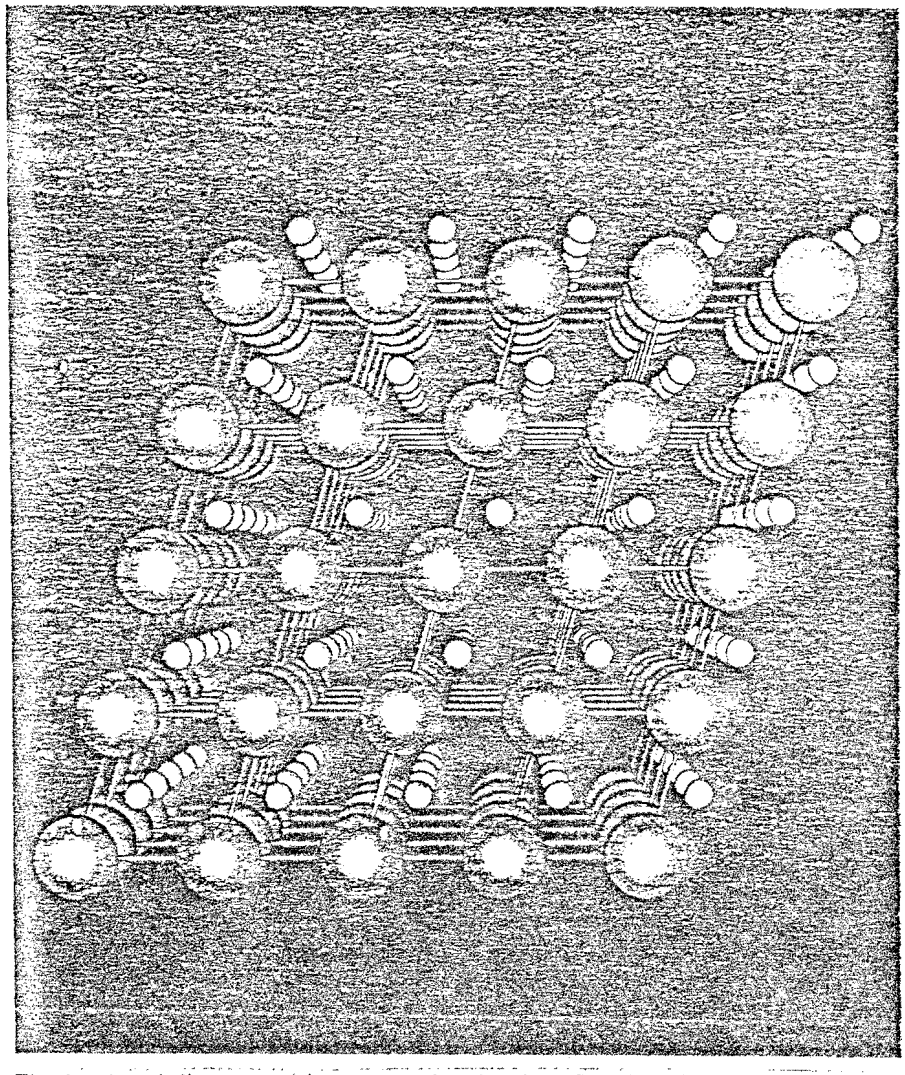

Fig. 1. A periodic two-particle system undergoing shear flow. For clarity the two particles have been drawn as hard spheres with two different diameters. 125 periodic repetitions of the shearing unit cell are shown.

Typical modifications include "driving forces" which generate fluxes, as well as "damping forces," which absorb the flux-generated irreversible heat. These new methods do provide relatively efficient routes to transport coefficients and to the simulation of fluids[3] and solids[4] under extreme conditions, such as those prevailing in strong shock waves. At present the extension of thermodynamics and constitutive models to incorporate the new results is an active research area.[5]

The principal flows of interest to nonequilibrium molecular dynamics are shear flows, dilational flows, and the flow of heat. Shear flows have undergone the most intensive study. They have been generated by a variety of techniques.[6] Of these, those generating a homogeneous periodic flow (see Fig. 1) appear to be most efficient. No corresponding method for simulating heat flow was developed until 1982, when Evans and Gillan avoided the usual temperature and density gradients associated with isobaric heat flow and suggested two similar methods for driving a heat current by using an energy-sensitive external force. Evans and Gillan and Dixon applied these schemes[7] to Lennard-Jones models of triple-point liquid argon, obtaining relatively precise linear and nonlinear heat conductivities. The linear conductivities agreed well with experimental data and with estimates based on alternative inhomogeneous simulation results.[8]

In the present work we apply both the new (1982) Evans scheme and Gauss' venerable (1829) principle of least constraint to the heat flow problem. The formulation, simulation, and discussion of the resulting heat flows make up the following three sections of this paper.

2. FORMULATION

The heat flux vector Q represents the direction and magnitude of the flow; Q is measured as energy per unit area and unit time. Heat flux is to be measured in the "comoving" frame so that mass motion does not contribute to Q. Fourier's law relates Q to the temperature gradient ∇T through the heat conductivity κ:

$$Q \equiv -\kappa \nabla T \tag{1}$$

In the linear regime the dissipation associated with homogeneous heat flow in a volume V can be expressed in terms of the irreversible entropy production $\dot{S}$:

$$T\dot{S} = Q^2 V/\kappa T = \kappa(\nabla T)^2 V/T \tag{2}$$

Within strong shock waves fluids become anisotropic. Comoving measures of temperature parallel and perpendicular to the motion can differ by a

factor of 2 or more.[3] It is still possible to use Fourier's expression (1). To do so T must first be defined. The definition can be based on local angle-averaged velocity fluctuations $\langle \delta v^2 \rangle \equiv 3kT/m$. In this way the conductivity κ can be *defined* by (1) outside the linear regime. By contrast the entropy production defined by (2) has no obvious thermodynamic meaning under such conditions.

In the linear regime, heat flow is described by Fourier's law [Eq. (1)] with the limiting small-gradient value of the conductivity. The linear Green–Kubo approach to transport expresses the conductivity κ in terms of the time decay of equilibrium heat flux fluctuations:

$$\kappa \equiv (V/kT^2) \int_0^\infty \langle Q_x(0)\, Q_x(t) \rangle_{eq}\, dt \tag{3}$$

where the microscopic heat flux component Q_x has the form

$$Q_x V \equiv \sum \dot{x} \frac{1}{2} m\dot{r}^2 + \sum\sum \left(\frac{\dot{x}_i + \dot{x}_j}{2} \right) \phi_{ij} + x_{ij} \left(F_{ij} \cdot \frac{\dot{r}_i + \dot{r}_j}{2} \right) \tag{4}$$

The single sum runs over all N particles in the volume V. The double sum runs over all $N(N-1)/2$ *pairs* of particles. Evans demonstrated that a realistic heat flow is generated if the Newtonian forces derived from the pair potential $\phi_{ij}(|r_i - r_j|) = \phi(r_{ij})$ have added to them an

$$\Delta F = \lambda [\delta E + \delta P^\phi_{xx} V, \delta P^\phi_{xy} V, \delta P^\phi_{xz} V] \tag{5E}$$

If the power absorbed by this force, $v \cdot \Delta F = \lambda Q V$, is equated to the rate of irreversible heating from (2), $Q^2 V/\kappa T$, we find $Q = \kappa \lambda T$. Thus in the linear regime the conductivity κ is equal to the ratio $Q/\lambda T$. The extra force (5E) generates and maintains an average heat current Q_x consistent with the thermodynamic relation (2) above.

We use δ in (5E) and (5G) below to indicate instantaneous fluctuations of particles' contributions to the energy or to the pressure tensor relative to the mean energy and pressure-tensor contributions at that time. By imposing an additional velocity-dependent force to constrain the temperature or the energy, a steady flow can be maintained. The heat flux generated by the forces (5E) exists in the absence of a temperature gradient, eliminating most of the size dependence of the resulting conductivity. Evans' calculation of the conductivity for triple-point liquid argon demonstrates that this approach is correct and efficient.

An alternative to Evans' method can be based on Gauss' principle of least constraint. Gauss stated that constraints—constant heat flux is one—should be imposed by using the smallest possible forces. "Smallest

possible" means that the constraint force F_c added to each particle, to enforce a non-Newtonian constraint, must minimize $\sum F_c^2/2m$, where the sum runs over all particles. We show below that these constraint forces are generally *not* those which would do the *least work* necessary to enforce a constraint.

It should be pointed out that special constrained simulations and special external forces are analogous to laboratory experiments in which mechanical systems are coupled to electromagnetic and gravitational fields. Properly generalized, thermodynamics and hydrodynamics should apply to these specialized simulations. In extending linear hydrodynamics it is therefore important to understand schemes such as Evans' and Gauss'. Such schemes are also likely to stimulate numerical few-body models for linear and nonlinear transport coefficients.

The set of constraint forces which satisfies Gauss' principle for constant heat flow Q_x with no mass flow ($\sum F_c = 0$) resembles Evans' set of additional forces ΔF:

$$F_c = \lambda[\delta E + \delta P_{xx} V, \delta P_{xy} V, \delta P_{xz} V] \tag{5G}$$

But in (5E) λ was fixed, Q fluctuated, and only the potential contribution to the pressure tensor was included. In (5G) λ varies with time, $Q_x V$ is fixed, and *total* pressure tensor contributions are included. If the calculations are carried out "isothermally," with $\sum \frac{1}{2} m\dot{r}^2$ fixed, additional forces $-\zeta m\dot{r}$ must be added to (5G). The resulting constraint equations can be solved for λ and ζ:

$$\lambda = \left[(\dot{Q}_x V)_N \sum m\dot{r}^2 + \left(Q_x V + \sum \dot{x} m\dot{r}^2 \right) \dot{\Phi}_N \right] \Big/ D \tag{6}$$

$$\zeta = \left[(\dot{Q}_x V)_N \left(Q_x V + \sum \dot{x} m\dot{r}^2 \right) + \sum H\, \delta H\, \dot{\Phi}_N \right] \Big/ D \tag{7}$$

where $(\dot{Q}_x V)_N$ is the rate at which $Q_x V$ would change with time using Newton's equations of motion and $\dot{\Phi}_N$ is the Newtonian rate of change of the total potential energy. The sum $\sum H\, \delta H$ and denominator D are as follows:

$$\sum H\, \delta H \equiv \sum \{[E + P_{xx} V][\delta E + \delta P_{xx} V] + [P_{xy} V][\delta P_{xy} V] + [P_{xz} V][\delta P_{xz} V]\} \tag{8}$$

$$D \equiv \left(Q_x V + \sum \dot{x} m\dot{r}^2 \right)^2 - \sum H\, \delta H \sum m\dot{r}^2 \tag{9}$$

Thus, for large systems, the only difference between Evans' and Gauss' approaches lies in the *kinetic* contribution to the additional forces

$$\lambda[(m\dot{x}\dot{x} - \langle m\dot{x}\dot{x}\rangle), m\dot{x}\dot{y} - \langle m\dot{x}\dot{y}\rangle, m\dot{x}\dot{z} - \langle m\dot{x}\dot{z}\rangle]$$

It is possible to show that *both* approaches (5E) and (5G) agree with the Boltzmann-equation conductivity in the low-density limit, where $\lambda_{\text{Evans}} \to 3\langle\lambda_{\text{Gauss}}\rangle$. At high density, where the kinetic contribution is relatively small, a comparison of scheme (5G) with (5E) would be inconclusive. In the next section we therefore consider a *relatively* low-density situation, in which the kinetic and potential parts of the heat flux are comparable in size. This state has already been characterized independently in Ashurst's thesis.[8] The same combination of density and temperature nearly coincides with a highly nonequilibrium shock wave state described in Ref. 3.

3. SIMULATION

We study 108 soft spheres interacting with the nearest-image pair potential,

$$\phi(r) = \varepsilon(\sigma/r)^{12} \tag{10}$$

in a periodic cubic box of volume V. The velocities sum to zero and the second moment is fixed by the thermodynamic temperature T:

$$\sum \tfrac{1}{2}mv^2 \equiv \tfrac{3}{2} \times 108kT \tag{11}$$

Ashurst measured the compressibility factor, shear viscosity, and heat conductivity at reduced fluid-phase densities

$$\frac{N\sigma^3}{\sqrt{2}\,V}\left(\frac{\varepsilon}{kT}\right)^{1/4} \equiv x = 0.4, 0.6, 0.7, 0.8 \tag{12}$$

The reduced density x at which soft spheres freeze is 0.813. We choose to compare the two schemes at the lowest of these fluid densities, 0.4, because the kinetic heat flux contribution $\sum \dot{x}mr^2/2V$ is relatively large, about half the potential contribution. This state also corresponds roughly to the center of a dense-fluid shockwave linking triple-point liquid argon to twofold compressed argon at 12,000 K.[3]

First, we used Evans' scheme, over a wide range of fluid and solid densities, varying the driving force constant λ. We list the results in Table I. Both the conductivities and the pressure data are nicely consistent with

Ashurst's for the densities in (12) above. See Fig. 2 for a least-squares fit (cubic in λ and x) of our data. The conductivity data for $\lambda \to 0$ can be roughly described by Ashurst's fit[8]:

$$\kappa\sigma^2(m/\varepsilon)^{1/2}(\varepsilon/kT)^{2/3}/k = 0.642 + 0.42[\exp(4.1x) - 1] \tag{13a}$$

where x is the reduced density defined in (12). A considerably better description is the cubic:

$$\kappa\sigma^2(m/\varepsilon)^{1/2}(\varepsilon/kT)^{2/3}/k = 0.642 + 2.5x^2 + 18x^3 \tag{13b}$$

At the reduced density 0.4 the *kinetic* part of the heat flux, $\sum \dot{x}m\dot{r}^2/2V$, slightly exceeds that predicted by the low-density Boltzmann equation conductivity $\kappa(\rho \to 0) = 0.642(kT/\varepsilon)^{2/3}\sqrt{\varepsilon/m}k/\sigma^2$. The Boltzmann estimate gives an approximate ratio (kinetic/potential) $0.642/(2.5\text{–}0.642) = 0.34$, agreeing with the small-lambda ratio listed in Table I.

Next we studied this *same* thermodynamic state (0.4) using Gauss' scheme, fixing the heat flux at the value given by Evans' scheme for $\lambda_E = 0.15$ and 0.30, and measuring the time average $\langle\lambda_G\rangle$. See Table II. In these calculations we removed the slow numerical drifts in Q_x and T (in the fifth or sixth figure) by rescaling the x velocities to restore $Q_x V$ to its desired value and rescaling the y and z velocities to restore the temperature. Three or four iterations of the form $\{v_x' = (1 + \varepsilon_x)v_x;\ v_y' = (1 + \varepsilon_y)v_y;\ v_z' = (1 + \varepsilon_y)v_z\}$ converged to fixed (to fourteen digits) $\{v'\}$. The rescaling was carried out at reduced time intervals of 1 or 5, roughly every thousand time steps. Although the programming of $(\dot{Q}_x V)_N$ is intricate, the constraints of fixed flux and temperature are powerful checks. The entire program was completed in about 40 hr. The values found in Table II suggest that Gauss' conductivity is lower than Evans' (correct) value and that Gauss overemphasizes the kinetic part of the heat flux. The reasons for the failure of Gauss' approach are outlined at length in the Discussion (Section 4) below.

Our Table I results for $(N\sigma^3/\sqrt{2V})(\varepsilon/kT)^{1/4} = 0.4$ indicate that the conductivity and the temperature and pressure anisotropicities induced by heat flow are highly nonlinear (roughly $\sim\lambda^3$). The temperature ratios T_{xx}/T_{yy} are 1.18, 1.55, and 2.44 for $\lambda = 0.4$, 0.6, and 0.8. The corresponding pressure ratios P_{xx}/P_{yy} are 1.04, 1.13, and 1.30. The strong Lennard-Jones potential shock-wave state from Ref. 3, at reduced densities and temperatures of 1.098 and 67, respectively, corresponds roughly to a soft sphere state with $(N\sigma^3/\sqrt{2V})(\varepsilon/kT)^{1/4} = 0.38$. The heat flux for this state corresponds roughly to a soft sphere value of $\lambda\sigma(\varepsilon/kT)^{1/12} = 0.7$. The nonlinear anisotropicies mentioned above are fully consistent with the temperature ratio 2.0 in the shock-wave and also account for most of the increase, relative to the

Table I. Compressibility Factor PV/NkT, Heat Conductivity κ, and Ratio of Kinetic to Potential Heat Flux as Functions of ρ and λ Using Evans' Method for 108 Soft Spheres for Various Reduced "Densities," $\rho = (N\sigma^3/\sqrt{2}V)(\epsilon/kT)^{1/4}$ [a]

ρ	$\lambda/T^{-1/12}$	$tT^{-7/12}$	PV/NkT	$\kappa/T^{2/3}$	Q_k/Q_e
0.8[b]	0.05	240	16.52	9.5	0.081
0.8[b]	0.10	240	16.52	10.3	0.084
0.8[b]	0.15	240	16.53	10.0	0.087
0.8[b]	0.20	240	16.50	11.1	0.093
0.8[b]	0.30	240	16.47	12.5	0.096
0.9[b]	0.03	240	22.53	16.1	0.074
0.9[b]	0.05	240	22.53	15.2	0.066
0.9[b]	0.07	240	22.53	16.9	0.068
0.9[b]	0.10	240	22.52	17.3	0.064
0.9[b]	0.15	240	22.53	18.7	0.066
0.9[b]	0.20	240	22.50	25	0.072
0.9[b]	0.30	240	22.37	36	0.085
1.0[b]	0.03	1520	30.96	30	0.044
1.0[b]	0.05	240	30.96	32	0.045
1.0[b]	0.07	240	30.96	34	0.046
1.0[b]	0.10	240	30.93	61	0.053
1.0[b]	0.15	240	30.85	90	0.062
1.0[b]	0.20	240	30.80	80	0.066
1.0[b]	0.30	240	30.74	57	0.072
0.1	0.02	2000	1.449	0.66	3.75
0.1	0.05	540	1.450	0.73	4.03
0.1	0.07	240	1.452	0.87	5.02
0.1	0.10	240	1.446	1.00	4.79
0.1	0.15	240	1.442	1.80	5.33
0.2	0.05	240	2.13	1.09	1.60
0.2	0.07	240	2.12	0.89	1.53
0.2	0.10	500	2.13	1.01	1.50
0.2	0.15	240	2.13	1.03	1.57
0.2	0.20	240	2.12	1.26	1.68
0.3	0.05	900	3.12	1.53	0.75

three

[a] The units of mass, length, and temperature are, respectively, m, σ, and ϵ/k. The steady-state fluid and solid simulations were carried out for total times t given in column two of the table. The compressibility factors $(PV/NkT \equiv (P_{xx} + P_{yy} + P_{zz})V/3NkT$ agree well with Ashurst's. At $\rho = 0.4$ he found $\kappa/T^{2/3} = 2.3 \pm 0.13$ and 2.1 ± 0.9 in calculations with equivalent $\lambda/T^{1/12}$ values of 0.008 and 0.028. The quoted pressures are reliable. The fluid-phase conductivities have uncertainties ranging from nearly 10% (small λ, $\rho \leqslant 0.4$) to about 1% (large λ, $\rho \geqslant 0.4$). The solid-phase conductivities have uncertainties ranging from near 10% (small λ, $\rho \geqslant 0.9$) to about 2% ($\lambda \sim 0.15$).

[b] Face-centered cubic solid.

Table continued

Table I. (Continued)

ρ	$\lambda/T^{1/12}$	$tT^{7/12}$	PV/NkT	$\kappa/T^{2/3}$	Q_λ/Q_0
0.3	0.10	240	3.13	1.57	0.73
0.3	0.15	240	3.11	1.53	0.73
0.3	0.20	240	3.13	1.60	0.70
0.3	0.30	240	3.11	1.89	0.82
0.4	0.05	450	4.58	2.54	0.38
0.4	0.10	240	4.58	2.23	0.36
0.4	0.15	240	4.57	2.24	0.38
0.4	0.20	240	4.57	2.35	0.37
0.4	0.30	240	4.57	2.49	0.40
0.4	0.40	240	4.56	2.65	0.41
0.4	0.60	240	4.46	4.27	0.66
0.4	0.80	240	4.24	6.89	0.95
0.5	0.05	468	6.64	3.47	0.21
0.5	0.10	240	6.63	3.65	0.21
0.5	0.15	240	6.63	3.55	0.20
0.5	0.20	240	6.64	3.62	0.21
0.5	0.30	240	6.62	3.74	0.22
0.6	0.05	240	9.52	5.09	0.103
0.6	0.10	240	9.52	5.54	0.116
0.6	0.15	240	9.51	5.52	0.14
0.6	0.20	240	9.51	5.36	0.13
0.6	0.30	240	9.50	5.59	0.14
0.7	0.05	2000	13.41	7.96	0.082
0.7	0.10	240	13.43	8.04	0.088
0.7	0.15	1000	13.42	7.88	0.086
0.7	0.20	240	13.43	7.92	0.091
0.7	0.30	240	13.42	7.78	0.091
0.8	0.03	500	18.61	11.05	0.070
0.8	0.05	240	18.60	11.40	0.073
0.8	0.10	240	18.61	10.50	0.062
0.8	0.15	240	18.62	10.69	0.060
0.8	0.20	240	18.64	10.37	0.061

Newtonian value, in the shock-wave shear stress. This nonlinear and nonreciprocal effect, shear stress resulting from heat flow, is the *only* effect so far characterized that accounts for the effective increase of viscosity in a strong shockwave. The other known effects—frequency, wavelength, and rate dependence of the shear viscosity—all predict decreases relative to the Newtonian value. For this reason further study of the coupling between momentum and energy flows is highly desirable.

Evans' scheme seems to work well in the anharmonic solid phase too. Provided that the solid-phase number dependence can be ignored, the results

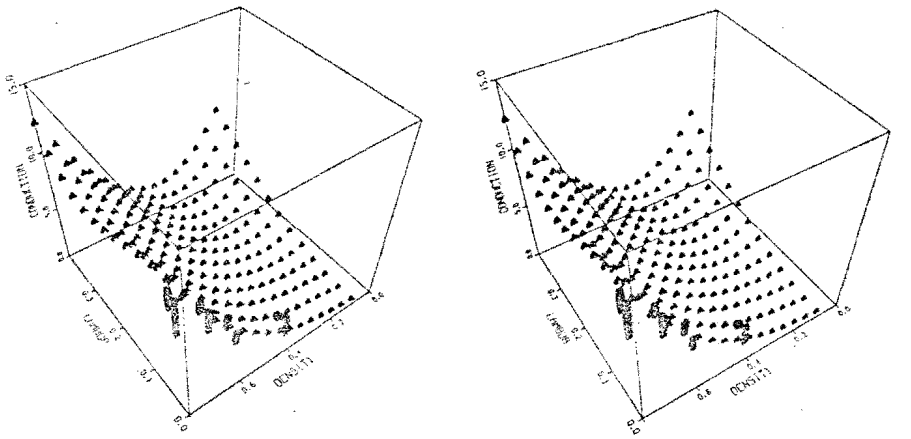

Fig. 2. Comparison of soft-sphere small-lambda fluid-phase thermal conductivities with Ashurst's values based on heat-reservoir simulation. The data exhibit overall consistency and approach the Boltzmann equation value at low density. The surface is a cubic Chebyshev least-squares fit of the fluid data in Table I. Ashurst's results, including error bars, are indicated by vertical heavy lines.

from Table I suggest that conductivities correct within 5% or so can be obtained. These conductivities can be compared with two different theoretical models. The simpler model[9] is based on energy transfer between adjacent planes of particles at a rate calculated from the Debye frequency. For the inverse twelfth power potential the Debye frequency varies as the 7/3 power of density. Including also the dependence of the interplanar spacing and temperature gradient on density leads to the prediction

$$\kappa\sigma^2(m/\varepsilon)^{1/2}(\varepsilon/kT)^{2/3}/k \doteq 20[\rho(\varepsilon/kT)^{1/4}]^{8/3} \qquad (14)$$

Table II. Compressibility factor PV/NkT, Heat Conductivity κ, and Ratio of Kinetic to Potential Heat Flux as Functions of $Q_x V$ using Gauss' Method for 108 Soft Spheres with $\rho = (N\sigma^3/\sqrt{2}V)(\varepsilon/kT)^{1/4} = 0.4$[a]

$Q_x V/T^{3/2}$	$\langle\lambda\rangle/T^{1/12}$	$tT^{7/12}$	PV/NkT	$\zeta/T^{7/12}$	$\kappa/T^{2/3}$	Q_y/Q_ϕ
68	0.104	250	4.58	0.04	1.9	0.60
143	0.200	240	4.56	0.16	2.1	0.60

[a] The units of mass, length, and temperature are, respectively, m, σ, and ε/k. The steady-state simulations were carried out for total times t given in column two of the table.

Three

This dependence on density is somewhat weaker than that indicated by the results in Table I. An alternative model considers anharmonic three-phonon interactions.[10] This model should be most accurate at high density, and leads to the result

$$\kappa\sigma^2(m/\varepsilon)^{1/2}(\varepsilon/kT)^{2/3}/k \doteq 28[\rho(\varepsilon/kT)^{1/4}]^{20/3} \tag{15}$$

This dependence is stronger than that found in Table I. We hope to carry out a more definitive solid phase study of number dependence in the future in order to determine the range of validity of the anharmonic theory.

4. DISCUSSION

The failure of Gauss' principle to reproduce the linear-regime dissipation predicted by irreversible thermodynamics indicates that specifying the comoving momentum and energy fluxes (P and Q) and thermodynamic state (ρ and T) is an incomplete description of the hydrodynamic states studied here. The difficulty lies in the rapid coupling of kinetic heat flow $Q_k = [\sum \frac{1}{2}\dot{x}m\dot{r}^2]/V$ and potential heat flow $Q_\phi = [\sum\sum \langle\dot{x}\rangle\phi + \dot{x}F \cdot \langle r\rangle]/V$. These variables are not "slow" variables in the absence of supporting gradients. By fixing the *ratio* of Q_k and Q_ϕ, the correct linear-regime thermodynamic dissipation

$$T\dot{S} = (Q_k + Q_\phi)^2 V/\kappa T \tag{16}$$

can indeed be reproduced, *but* the resulting conductivity, κ, will only be *correct* if the initial ratio Q_k/Q_ϕ is also correct. Gauss provides no *a priori* prediction of this ratio.

In the linear regime the error inherent in Gauss' principle can be analyzed by using linear-response theory. An initial canonical phase-space density $f_0 \sim \exp[-E/kT]$ varies with time when Evans' ($\alpha = 1$) or Gauss' ($\alpha = 3$) heat-flux schemes are used:

$$\ln\left(\frac{f}{f_0}\right) = \left(\frac{\lambda V}{kT}\right)\int_0^t (\alpha Q_k + Q_\phi)_s\, ds \tag{17}$$

Thus the average steady heat flux is different in the two schemes:

$$Q = \left(\frac{\lambda V}{kT}\right)\int_0^\infty \langle (Q_k + Q_\phi)_0 (\alpha Q_k + Q_\phi)_t \rangle_{eq}\, dt \tag{18}$$

Likewise, the irreversible heating differs:

$$T\dot{S} = \lambda V \langle \alpha Q_k + Q_o \rangle_{ne}$$

$$= (\lambda^2 V^2/kT) \int_0^\infty \langle (\alpha Q_k + Q_o)_0 (\alpha Q_k + Q_o)_t \rangle_{eq} \, dt \tag{19}$$

Finally, using the connection (2) between conductivity and irreversible heating,

$$\kappa T = Q^2 V / T\dot{S} \tag{2}$$

we can express the ratio of Evans' conductivity to Gauss'; in terms of the three heat current correlation functions we have

$$\frac{\kappa_E}{\kappa_G} = \frac{\int \langle (Q_k + Q_o)_0 (Q_k + Q_o)_t \rangle \, dt \int \langle (3Q_k + Q_o)_0 (3Q_k + Q_o)_t \rangle \, dt}{[\int \langle (3Q_k + Q_o)_0 (Q_k + Q_o)_t \rangle \, dt]^2} \tag{20}$$

This ratio can be estimated using Enskog's approximate hard-sphere theory of dense-fluid transport,[11] with the result

$$\frac{\kappa_E}{\kappa_G} \doteq \frac{(1 + 1.2y + 0.755y^2)(9 + 3.6y + 0.755y^2)}{(3 + 2.4y + 0.755y^2)^2} \tag{21}$$

The error in the Gauss' principle conductivities from Eq. (18) is too small. This shows that Enskog theory predictions are inaccurate for soft spheres. Enskog theory predicts a kinetic heat flux proportional to $0.6 + y^{-1}$. This corresponds to a factor-of-2 variation in kinetic heat flux along a fluid-phase isotherm. In fact, the kinetic contribution is nearly constant, equal to the low-density Boltzmann-equation value.

For a soft-sphere fluid Enskog's effective hard-sphere compressibility factor, $PV/NkT = 1 + y$, varies between 1 and 7. The maximum value of the ratio (21), 1.0540, occurs at $y = 1.993$, close to the value $y = 1.837$ corresponding to reduced density 0.4 studied in Section 3. The predicted ratio at $y = 1.837$ from (18), 1.0538, is considerably less than 1.2, the molecular dynamics result. Thus the linear conductivity can be in error by as much as twenty percent if Gauss' principle is used.

Although Gauss *does* minimize the rms constraint force, he does not minimize the work of constraint. Thus $T\dot{S}/V = 0.056$ and 0.224 for Evans' method with $\langle Q_x V \rangle = 68$ and 143. For Gauss' slightly larger losses result, 0.063 and 0.265, respectively.

In almost all situations Gauss' principle is precisely equivalent to Newtonian mechanics. But for inhomogeneous nonlinear nonholonomic constraints, Gauss' principle goes beyond Newton. We have here a concrete

case—the only one known so far—in which the use of Gauss' principle produces false results.

The failure arises for two reasons. First, the kinetic and potential parts of the heat flux are, respectively, cubic and linear in the particle velocities. Second, the equilibrium decay rate of the flux is not sufficiently slow, relative to the kinetic-potential interconversion time.

There seems to be no analog of the Evans–Gillan scheme applicable to the measurement of viscosity. In the viscous case the kinetic and potential parts of the stress are quadratic and zeroth-order functions of velocity. Because the potential contribution is velocity independent it is necessary to use periodic deforming boundaries to drive that part of the viscous stress.

REFERENCES

1. W. G. Hoover, *Ann. Rev. Phys. Chem.* 34:103 (1983).
2. D. Levesque, L. Verlet, and J. Kurkijarvi, *Phys. Rev.* 7A:1690 (1973).
3. B. L. Holian, W. G. Hoover, B. Moran, and G. K. Straub, *Phys. Rev.* 22A:2798 (1980).
4. A. J. C. Ladd and W. G. Hoover, *Phys. Rev.* 28B:1756 (1983).
5. See, for instance, International Seminar on Recent Developments in Nonequilibrium Thermodynamics—Barcelona, Spain—26–30 September 1983, to be published by Springer Verlag.
6. W. G. Hoover, *Physica* 118A:111 (1983); for a comprehensive clear review, see D. J. Evans and G. P. Morriss, Non-Newtonian Molecular Dynamics, to appear in *Computer Phys. Rep.*
7. D. J. Evans, *Phys. Lett.* 91A:457 (1982); M. J. Gillan and M. Dixon, *J. Phys. C:Solid State Phys.* 16:869 (1983).
8. W. T. Ashurst, Dense Fluid Shear Viscosity and Thermal Conductivity via Non-Equilibrium Molecular Dynamics, Ph.D dissertation, University of California at Davis (1974); W. T. Ashurst, Determination of Thermal Conductivity Coefficient via Non-Equilibrium Molecular Dynamics, in *Advances in Thermal Conductivity*, R. L. Reisbig and H. J. Sauer, eds., Proc. Intl. Conf. on Thermal Conductivity (Lake Ozark, Missouri, November 5–7, 1973).
9. See the references to the Horrocks, McLaughlin, Andrade model cited in Ashurst's Ref. 8.
10. See, for instance, P. G. Klemens, *High Temp. High Pressure* 15:249 (1983).
11. J. O. Hirschfelder, C. F. Curtiss, and R. B. Bird, *Molecular Theory of Gases and Liquids* (Wiley, New York, 1954), pp. 647, 649.